

Structural Insight on the Activity of Type 1 Angiotensin II Peptide Antagonists Using MD Simulations

Marco A. C. Preto,[‡] André Melo,[†] Lígia M. Rodrigues,[‡] Hernâni L. S. Maia,[‡] and Maria J. Ramos^{*,†}

REQUIMTE, Departamento de Química, Faculdade de Ciências, Universidade do Porto, Rua do Campo Alegre, 687, 4169-007 Porto, Portugal, and Departamento de Química, Universidade do Minho, Gualtar, 4710-057 Braga, Portugal

Received: March 11, 2008; Revised Manuscript Received: July 18, 2008

Angiotensin II (AngII) is an octapeptide hormone, which plays a very important role in the blood pressure control mechanism. The excess production of this hormone is one of the main causes of hypertension illness. The antagonists for AngII At1 receptor constitute some of the most effective antihypertension drugs. In this work, both tested type1 AngII antagonists as well as new modeled antagonists (obtained by substitution of nonspecific amino acids by noncode residues (Sarcosine (Sar) and several $C_{\alpha}C_{\alpha}$ -dialkylglycines)) were simulated in dimethyl sulfoxide (DMSO) using molecular dynamics (MD). A number of common structural characteristics were identified on the active (and potentially active) simulated analogs, which seem to be correlated with their antagonistic activity. Two of the designed analogs were proposed as possible antagonists.

Introduction

Many illnesses are related to excess production of bioactive peptides. In many cases the administration of appropriate antagonists can prevent the undesired action of the biomolecule produced in excess, by blocking the respective receptors.^{1,2}

AngII is an octapeptide (Asp1-Arg2-Val3-Tyr4-Ile5-His6-Pro7-Phe8) hormone, which undertakes a crucial role in the mechanism of blood pressure regulation. Its interaction with its At1 receptor is responsible for a series of physiological responses, which lead to the increase of blood pressure.^{2,3} Angiotensin converting enzyme (ACE) inhibitors and Renin inhibitors prevent the formation of AngII, by acting in its precursors cascade.^{4,5} On the other hand, AngII antagonists acting independently of AngII synthetic pathways allow a more effective blockage of the At1 receptor mediated effects related to the excess production of this hormone.^{4,5} Although the inhibitors that prevent AngII formation are more effective for a high-risk population, AngII antagonists have similar efficiency for long-term therapies with less significant side effects.^{6,7}

Commercially available AngII antagonists are non peptidic synthetic compounds.^{8,9} Although a large number of AngII antagonists have been tested since the late 1970s, only in the early 1990s had an effective nonpeptide antagonist (Dup753)¹⁰ been introduced by DuPont. After clinical trials, it resulted in Losartan the first commercially available nonpeptide AngII antagonist, which is a very popular and effective antihypertensive drug.⁶ The most important disadvantage of peptide AngII antagonists is associated with the fact that they can not be administered orally. In fact, they are decomposed by gastrointestinal enzymes and have short plasma lifetime.^{9,11} Patients have to be treated by injection, which is highly undesirable in the case of a chronic blood pressure illness. A possible methodology to circumvent this problem is to create peptomi-

metics AngII antagonists, generated by appropriate mutation of coded amino acids by noncoded ones,^{12–15} which preserve a high affinity to the At1 receptor, but are not recognized (or are only poorly recognized) by gastrointestinal enzymes. Significant evidence have been accumulated that polar and charged residues of AngII, such as Arg2, Tyr4, His6 and the terminal carboxyl group, are very important for binding with the At1 receptor.^{2,16–18} On the other hand, C-terminal residues (Tyr4, His6 and Phe8, together with the terminal carboxylate) are crucial for At1 receptor activation.^{2,16–18} Other important features have also been identified by structure activity studies, namely:

(a) The agonist behavior is strongly dependent on the nature of the residue in position 8. In fact, type 1 antagonist of AngII, characterized by slow receptor resensitization rates, can be obtained by the substitution of Phe8 by an aliphatic residue (Ile, Ala, etc).¹⁹ On the other hand, reversible type 2 antagonists can be produced by methylation of Tyr4 side chain.¹⁹

(b) The mutation of Asp1 by a nonpolar synthetic residue, such as Sarcosine (Sar), increases the activity of both agonist and antagonist analogs of AngII.^{19,20}

(c) Positions 3, 5, and 7 of AngII are nonspecific both for binding and activation. However, the residues at these positions are important to retain bioactive conformations of AngII analogs.¹¹ In this context, mutations of an original amino acid in any of these positions have been observed to be possible in potent antagonists of AngII.^{11,21}

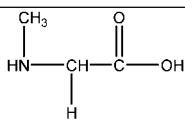
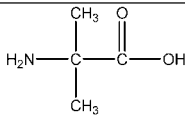
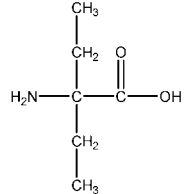
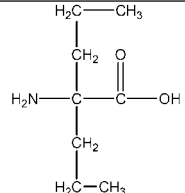
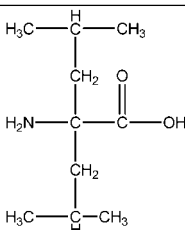
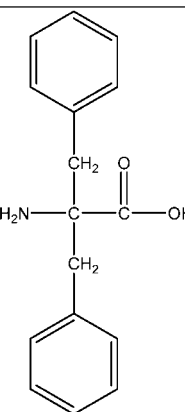
In this work, both well-tested AngII antagonists and new modeled potential antagonists of this hormone were simulated using MD simulations. Our modeling strategy was developed to generate new bioactive AngII (type 1) antagonist analogs, preventing the recognition of the peptide bonds by gastrointestinal enzymes. This strategy is based on the following: (a) mutation of Asp1 by Sar; (b) substitution of most of the original amino acids in nonspecific positions (Val3, Ile5 and Pro7) by appropriate noncoded residues; (c) substitution of Phe8 residue by an aliphatic residue (either Ile, or a α,α -dialkylglycine). The use of noncoded amino acids is known to reduce the peptide degradation speed by digestive enzymes.²² The noncoded amino

* Corresponding author. E-mail: mjrmos@fc.up.pt.

[‡] Departamento de Química, Universidade do Minho.

[†] REQUIMTE, Departamento de Química, Faculdade de Ciências, Universidade do Porto.

TABLE 1: Identification of the Non-Coded Amino Acids Used in This Work

Name	3 letter code	Structure	Availability
Sarcosine	Sar		Commercially available
Aminoisobutyric acid	Aib		
Diethylglycine	Deg		Prepared in Univ. of Minho (reference 12 and 13)
Dipropylglycine	Dpg		
Diisobutylglycine	Di,bg		
Dibenzylglycine	Db _n g		

acids used in this work (Sar and several C_{α},C_{α} -dialkylglycines) are either available commercially or are currently synthesized in the laboratories of University of Minho ^{12,13} (these noncoded amino acids are presented in Table 1). The main purpose of these simulations was to identify common structural features in an intermediate polarity moiety, which can be correlated with the activity of these biomolecules.

Simulation Details

A total number of 13 potential antagonists, in which some original coded amino acids were mutated by noncoded residues according to the methodology previously described, were designed. Additionally, 5 well-tested AngII antagonists^{21,23} were also studied. All simulated species were in their zwitterionic form. The list of all the AngII simulated analogs is presented in Table 2.

The conformational behavior of these molecules in a DMSO environment (which, being an intermediate polarity solvent, is believed to better mimic the receptor proximity) was studied using MD simulations. The Amber software package was used,²⁴ together with the Amber force field (parm99).^{25,26} DMSO was treated using the OPLS united-atoms potential parameters.²⁷ The parameters for the noncoded amino acids were established in a previous work.¹⁴ These parameters were established within an Amber force field methodology. Special care was taken during the parametrization of the charges, using a methodology that takes into account several structural minima, avoiding a strong dependence between structure and charges as these are very important in an intermediate polarity moiety.¹⁴ The initial structures for all the simulated species were obtained modifying the NMR AngII structure refined by Mavramoustakos and co-workers.²⁸

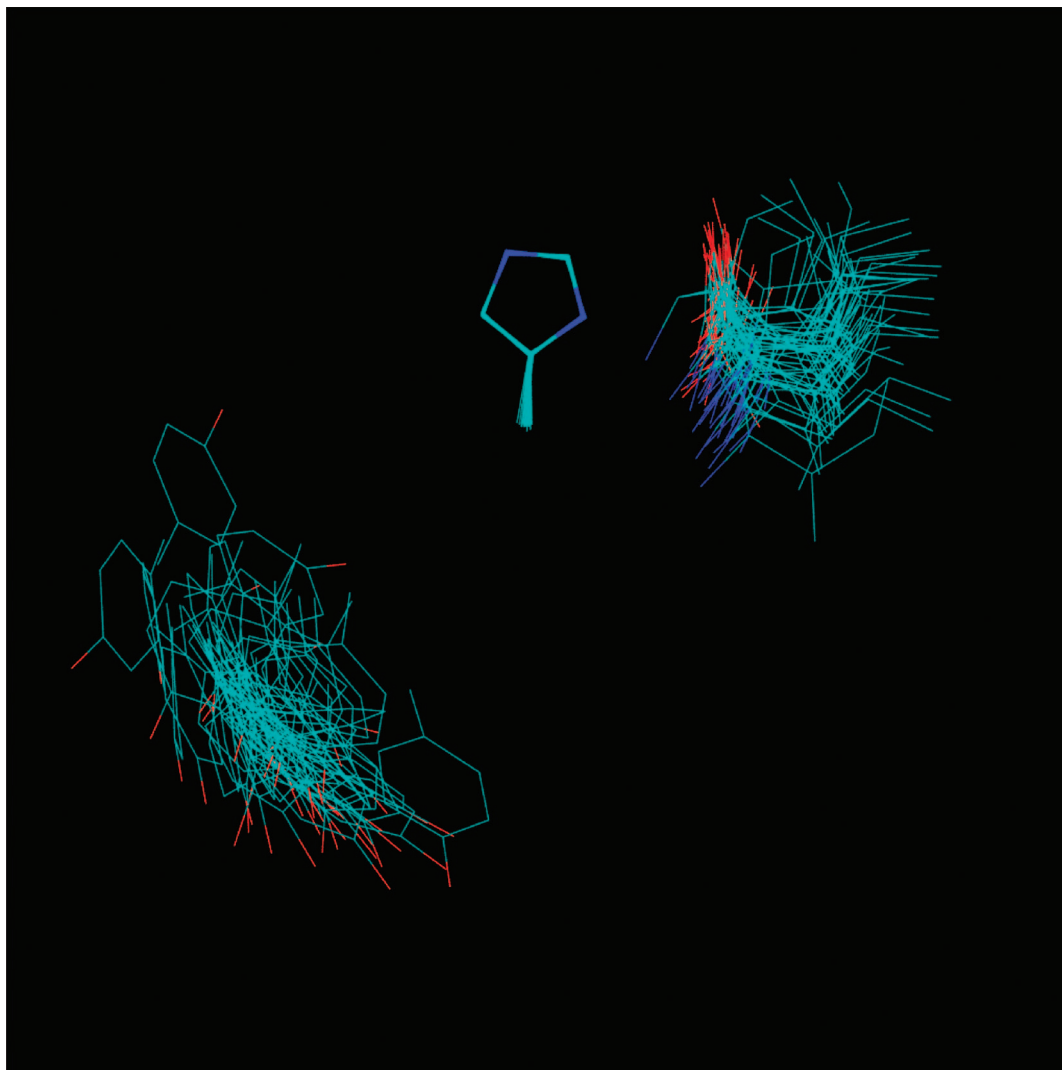


Figure 1. Superimposition of His6 side chain, also showing the Tyr4 side chain (lower left) and C-terminal residue (upper right). The frames were collected from the simulation of [Sar¹,Ile⁸]AngII, in intervals of 25 ps, showing the last 1.25 ns of the simulation. We can observe the relative arrangement of the Tyr4 side chain and the His6 side chain. Besides being very far apart, the majority of the simulation puts these two side chains oriented apart from each other. We can also note the presence of a hydrogen bond between the N_δH of His6 and the terminal carboxylate of Ile8.

TABLE 2: Average RMSD (Root-Mean-Square Deviation) and Standard Deviation of the Backbone Atoms of Each Simulation (Calculated for the Hole Backbone, for the N-Terminal Region (Res. 1 to Res. 4) and for the C-Terminal Region (Res. 5 to Res. 8))

	all backbone		N-terminal region		C-terminal region	
	av	std dev.	av	std dev	av	std dev
AngII	1.156	0.495	0.733	0.289	0.264	0.094
[Sar ¹ ,Aib ³ ,Ile ⁸]AngII	2.285	0.228	0.962	0.188	0.447	0.186
[Sar ¹ ,Aib ⁵ ,Ile ⁸]AngII	2.485	0.252	0.868	0.213	0.369	0.263
[Sar ¹ ,Aib ⁷ ,Ile ⁸]AngII	1.877	0.518	1.006	0.229	0.325	0.092
[Sar ¹ ,Aib ⁸]AngII	3.017	0.131	0.920	0.249	0.514	0.072
[Sar ¹ ,Ile ⁸]AngII	2.394	0.271	0.924	0.184	0.724	0.162
Comp 1 [Sar ¹ ,Aib ³ ,Aib ⁵ ,Aib ⁸]AngII	2.434	0.647	1.367	0.296	0.837	0.224
Comp 2 [Sar ¹ ,Dpg ⁸]AngII	1.414	0.363	0.903	0.183	0.383	0.173
Comp 3 [Sar ¹ ,Deg ⁸]AngII	1.711	0.410	0.999	0.298	0.903	0.087
Comp 4 [Sar ¹ ,Dibg ⁸]AngII	2.174	0.186	0.556	0.171	1.355	0.155
Comp 5 [Aib ³ ,Aib ⁵ ,Aib ⁸]AngII	1.913	0.389	0.885	0.232	0.670	0.076
Comp 6 [Sar ¹ ,Dbn ⁸]AngII	2.183	0.374	0.933	0.223	0.466	0.187
Comp 7 [Sar ¹ ,Deg ³ ,Deg ⁵ ,Deg ⁸]AngII	1.493	0.243	1.329	0.128	0.317	0.118
Comp 8 Sar ¹ ,Dpg ³ ,Dpg ⁵ ,Dpg ⁸]AngII	2.651	0.302	0.878	0.199	1.040	0.103
Comp 9 [Sar ¹ ,Deg ³ ,Aib ⁵ ,Deg ⁸]AngII	2.382	0.481	1.387	0.206	0.355	0.100
Comp 10 [Sar ¹ ,Deg ³ ,Aib ⁵ ,Aib ⁸]AngII	2.150	0.593	0.836	0.210	0.327	0.095
Comp 11 [Sar ¹ ,Dpg ³ ,Aib ⁵ ,Dpg ⁸]AngII	2.396	0.237	0.904	0.196	0.462	0.095
Comp 12 [Sar ¹ ,Deg ³ ,Aib ⁷ ,Ile ⁸]AngII	2.665	0.196	1.064	0.201	1.341	0.117
Comp 13 [Sar ¹ ,Deg ³ ,Aib ⁵ ,Dpg ⁸]AngII	2.355	0.286	0.928	0.212	0.268	0.061

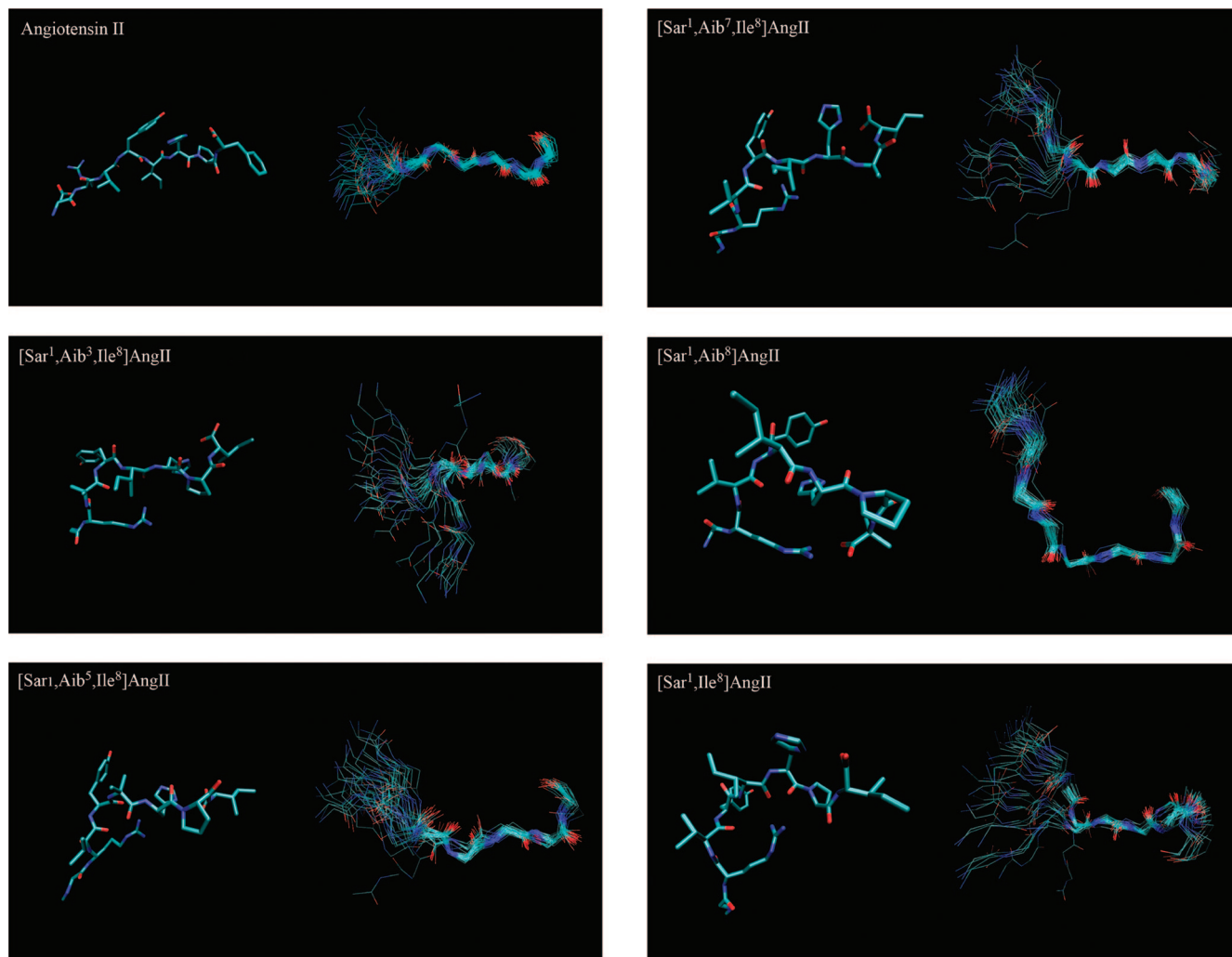


Figure 2. Minimal energy structure and backbone conformations of each of the simulated antagonists (backbone atoms from residue 4 to residue 6 were used to superimpose the backbone structures).

These structures were inserted in a pre-equilibrated DMSO cubic box, created with PAKMOL software.²⁹ The number of DMSO molecules included in each MD simulation varied from 908 to 1393 and the side length of the DMSO box varied from 51.04 Å to 59.25 Å. Cl[−] anions were used to neutralize the systems when this was necessary. These anions were placed within 4 Å of the charged amino terminal group. Solvent molecules were deleted, when the distance between one of their atoms and any solute atom was lower than the sum of their respective van der Waals (VDW) radii.

Each initial structure was then minimized, until the root-mean-square energy gradients were lower or equal to 0.001 kcal mol^{−1}, using 10 steps of steepest descent and performing a maximum of 190 steps using the conjugated gradients method. The solute structure remained frozen during these minimizations, in order to optimize the solvent distribution. All the systems were subsequently equilibrated at 300 K in a canonical (*NVT*) ensemble, using the Berendsen temperature coupling method³⁰ with a coupling constant of 1.0 ps. A harmonic constrain of 1 kcal mol^{−1} were applied to all solute atoms. A short equilibration in *NPT* ensemble was also carried out, during 20 ps. The production simulations were then performed, in a *NPT* ensemble, for 2 ns each. All *NPT* simulations were carried out at 300 K and 1 atm, using the Berendsen thermostat and barostat³⁰ with coupling constants of 1.0 and 0.2 ps respectively.

All molecular simulations were carried out using periodic boundary conditions (PBC). The equations of motion were

integrated every 1 fs using the Verlet leapfrog algorithm³¹ and SHAKE constraints³² were applied to all bonds connecting hydrogen and heavy atoms. Long range interactions were estimated using the particle mesh Ewald (PME) method^{33,34} for the electrostatic component and a continuum model was used for the VDW component. A distance cutoff of 12 Å, with a skin of 2 Å, was used to generate the list of non bond pairs, which was updated whenever any atom was moved more than 1 Å from the last position. Long range electrostatic interactions were truncated at cutoff plus skin distance and VDW and 1–4 electrostatic interactions were truncated at cutoff distance. 1–4 VDW interactions were scaled down by a factor of 2 and 1–4 electrostatic interactions were scaled down by a factor of 1.2. Structural and thermodynamic quantities were stored every 50 steps (0.050 ps) for further analysis.

All simulations were carried out in a dual Pentium IV Xeon computer. The three-dimensional images, presented in this work, were generated using the VMD package.³⁵

Results

In our previous work on the structure of AngII in both water and DMSO solution, several key structural features were identified:³⁶ (a) the N-terminus of AngII is considerably more flexible than its C-terminus; (b) a hydrogen bond is present between a hydrogen of the Histidine's imidazol side chain and one oxygen of the terminal carboxylate; (c) a spatial proximity

TABLE 3: Specific Features of AngII, Its Type 1 Antagonists and Designed Analogs (the Gray Shaded Lines Show the Most Promising Candidates)^a

peptide	C-terminus rigidity	orientation in different directions of Tyr4 and his 6 side chains ^b	formation of hydrogen bond between His6 side chain and the terminal carboxylate	disruption of the salt-bridge identified in AngII, between Residue 1 and Arg2	common orientation of the C-terminal region when superimposing the N-terminal region ^c
AngII	+	><	+	—	AngII
[Sar1,Aib3,Ile8]AngII	+	<>	+	+	type 1 ant
[Sar1,Aib5,Ile8]AngII	+	<>	+	+	type 1 ant
[Sar1,Aib7,Ile8]AngII	+	<>	+	+	type 1 ant
[Sar1,Aib8]AngII	+	<>	—	+	type 1 ant
[Sar1,Ile8]AngII	+	<>	+	+	type 1 ant
Comp 2	+	><	+	+	AngII
Comp 3	—	<>	—	+	X
Comp 4	—	><	—	+	type 1 ant
Comp 5	+	><	+	+	AngII
Comp 6	+	<>	+	+	type 1 ant
Comp 7	+	><	+	+	X
Comp 8	—	<>	—	+	type 1 ant
Comp 9	+	<>	+	+	X
Comp 10	+	<>	+	+	X
Comp 11	+	<>	+	+	type 1 ant
Comp 12	—	><	—	+	type 1 ant
Comp 13	+	<>	+	+	type 1 ant

^a The symbol + indicates that the peptide presents the correspondent feature, while the symbol - has the opposite meaning. ^b The notation (><) indicates that Tyr4 and His6 aromatic side chains are oriented toward each other, where the symbol (<>) indicates that these side chains are oriented in opposite direction. ^c The notation (AngII) indicates that, when superimposing the N-terminal region, the C-terminus region has a similar orientation to AngII, the notation (Type 1 ant) indicates that this feature is similar to the structural motif presented by AngII type 1 antagonists, and the notation (X) indicates that the structure presented by the peptide is different both from AngII and its type 1 antagonists.

between the Tyr4 and His6 side chains is observed (however, no hydrogen bond is identified between atoms of these two residues); (d) a salt bridge involving Asp1 and Arg2 side chains can be found; (e) a slight bend occurs at residue Tyr4.

The simulations performed on the known peptide AngII At1 antagonists show differences and similarities of behavior in relation to AngII, which seem to be correlated with their activity. The following points are generally considered. (a) The C-terminal region undertakes an essential role in the biological activity, both for agonistic and antagonistic activity.^{18,37} The lower root-mean-square deviations (rmsd) found for the C-terminal region (when compared to the N-terminal one), as can be observed in Table 2, seem to reflect its high specificity. (b) The clustering of Tyr4 and His6 side chains does not seem to be mandatory for antagonistic activity (Figures 1 and 2). In fact, the proximity between Tyr4 and His6 is not usually observed, as these groups were generally oriented in different directions, whereas in AngII they are pointing toward each other. Figure 1 shows a representative example of the kind of relative disposition found for these two side chains. (c) The formation of a hydrogen bond between the imidazol's Nδ and one of the two terminal carboxylate oxygens, seem to be essential for antagonistic activity (all but one simulated known antagonists ([Sar1,Aib8]AngII) have clearly shown this interaction—Table 3). A representative example is presented in Figure 1. However, our results also suggest a different binding mode for the C-terminal region, when comparing with AngII (Figure 3). (d) Previous works have shown that the substitution of Asp1 by Sar improves both agonist and antagonist activity.^{19,20} We believe that this is a result (at least in part) of the disruption of the salt-bridge previously identified in AngII,³⁶ between the side chains of residue 1 (Asp) and 2 (Arg). This suggests that the guanidinium group of Arg2 side chain can establish an attractive interaction with a specific region of the receptor, increasing the affinity of the analogs that have a “free” Arg2 (whose side chain is not

involved in a strong interaction). (e) The comparison of the minimal energy backbone structure of AngII and the simulated Antagonists, revealed a striking feature: the slight bent that occurs in AngII, around residue 4, is different in all the simulated antagonists. On these antagonists, this bend is much more pronounced, resulting from the combinations of the backbone dihedrals from residue 4 and 5, as can be seen in figure 3. This resulted in a common feature to all simulated antagonists. When superimposing their N-terminal portion, all the simulated antagonists shared a similar orientation of the C-terminal region (very distinct from the orientation found for AngII), which is in accordance with the proposed activations model by Wilkes et al.,¹⁸ in which AngII and its type I antagonists share the same binding mode on the N-terminal region and differ on the C-terminal (moving the C-terminal carboxylate away from its interacting point and thus avoiding the receptor activation).

The designed candidates for type 1 antagonist activity were qualitatively analyzed, according to the specific features identified in the simulations for well-known type 1 antagonists (Table 3), enabling us to rule out some of the candidates in order to select a set of the more promising ones. To further narrow this number, an additional characteristic was taken into account: the predictable resistance to digestion of the newly designed compounds. This feature is strongly correlated with the number of noncoded residues. This can be obtained by increasing the number of substitutions of nonspecific amino acids by the noncoded ones, thus increasing the number of “strange” peptide bonds to the gastrointestinal enzymes. With this methodology, a high affinity to the At1 receptor can be conjugated with a poor recognition of the designed peptide by the mentioned enzymes.

In this context, Comp 11 ([Sar1,Dpg3,Aib5,Dpg8]AngII) and 13 ([Sar1,Deg3,Aib5,Dpg8]AngII) present all the specific features identified for type 1 antagonistic activity (Figure 4) and, having a considerable number of substitutions, are predicted to have a slow degradation rate by gastrointestinal enzymes

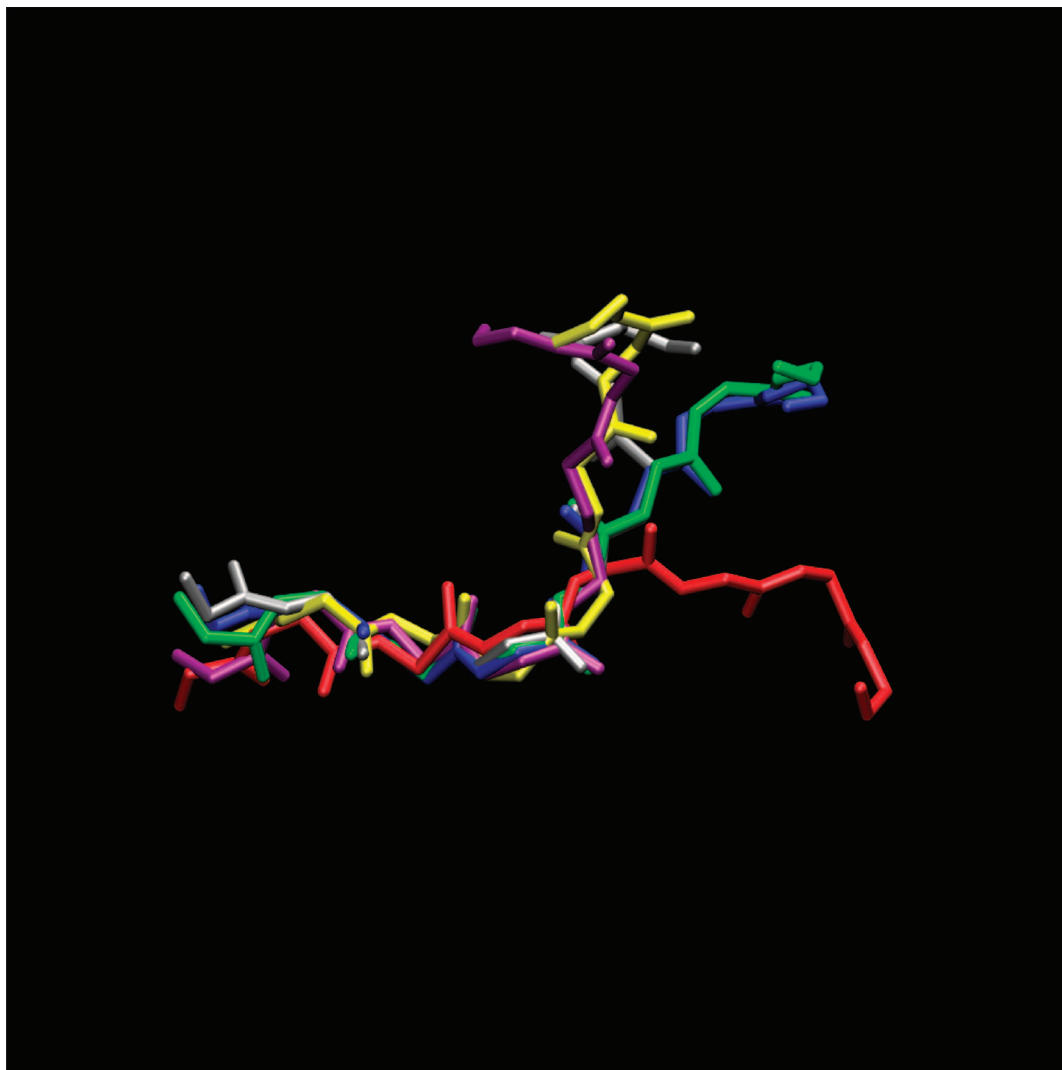


Figure 3. Superimposition (only peptide backbone shown) of the N-terminal region of AngII and the simulated known type 1 Antagonists (the found minimum energy conformers were used for the superimposition and the AngII structure was used as reference). AngII is represented in red, [Sar¹, Aib³, Ile⁸]AngII in Blue, [Sar¹, Aib⁵, Ile⁸]AngII in yellow, [Sar¹, Aib⁷, Ile⁸]AngII in green, [Sar¹, Aib⁸]AngII in purple and [Sar¹, Ile⁸]AngII in gray. A rough common motif for the antagonists is observed.

action. Consequently, they seem to be the best predictable candidates for efficient AngII type 1 antagonists.

The mutation of coded amino acids by noncoded α,α -dialkylglycines residues does not significantly affect the peptide backbone structure. In fact, the $C\alpha_i-C\alpha_{i+2}$ and the $C\alpha_i-C\alpha_{i+3}$ distances are not significantly altered by this type of substitution. Another important feature induced by these substitutions is a decrease of the backbone dihedral variability (Table 4). Although residue 2 increased its conformer number, we believe that this is a direct result from the disruption of the salt-bridge that constrained its backbone dihedral angles in the AngII. The decrease of backbone variability can be thermodynamically favorable for the peptide-At1 receptor association process, by decreasing the correspondent standard entropy variation.

A more complete set of collected data was supplied and is available as Supporting Information.

Conclusion

In this work, a set of specific features, responsible for type 1 antagonistic activity toward AngII At1 receptor, were proposed. These features were inferred from MD simulations of well-known peptide antagonists in DMSO.

New candidates, for peptidic type 1 antagonists of AngII, were also designed. These peptides were obtained by the mutation of nonspecific amino acids, in AngII sequence, by noncoded residues. Some of these synthetic residues are currently synthesized in the laboratories of the University of Minho.^{12,13} These designed analogs were studied using MD simulations, performed on DMSO, to select the candidates that present the specific features inferred from the well-known simulated type 1 AngII antagonists. The predictable resistance to digestion of these newly designed compounds, resulting from their poorer recognition by gastrointestinal enzymes, was also considered as an additional feature.

Two newly designed peptides, Comp 11 ([Sar¹,Dpg³,Aib⁵,Dpg⁸]AngII) and Comp 13 ([Sar¹,Deg³,Aib⁵,Dpg⁸]AngII), were proposed as good candidates to type 1 AngII antagonists. As can be observed in Figure 5, when their N-terminal backbone region for superimposition with AngII found minima, their N-terminal region is very similar (with the exception of the salt-bridge that can only be observed on AngII). Note that even the Tyrosine side chains occupy the same region (although only the backbone atoms were used for the superimposition). Furthermore, the introduction of α,α -Dialkylglycines in AngII



Figure 4. Superimposition of the N-terminal portions of minimal energy found structures of AngII (blue), known antagonists (red) and Comp 11, and 13 (yellow).

TABLE 4: Local Backbone Conformers of AngII, Comp 11 and Comp13, obtained by Molecular Dynamics Simulations*

AngII			Comp 11			Comp13		
residue	no. of conformers	characterization	residue	no. of conformers	characterization	residue	no. of conformers	characterization
Asp1	3	$\varphi \approx 55^\circ; \psi \approx 30^\circ$; $\varphi \approx 180^\circ; \psi \approx 30^\circ$; $\varphi \approx -65^\circ; \psi \approx 30^\circ$	Sar1	2	$\varphi \approx -40^\circ; \psi \approx 165^\circ$; $\varphi \approx -40^\circ; \psi \approx 120^\circ$	Sar1	2	$\varphi \approx 35^\circ; \psi \approx 160^\circ$; $\varphi \approx 35^\circ; \psi \approx 120^\circ$
Arg2	1	$\varphi \approx 50^\circ; \psi \approx -28^\circ$	Arg2	4	$\varphi \approx -80^\circ; \psi \approx 100^\circ$; $\varphi \approx -80^\circ; \psi \approx 140^\circ$; $\varphi \approx -170^\circ; \psi \approx 100^\circ$; $\varphi \approx -170^\circ; \psi \approx 140^\circ$	Arg2	2	$\varphi \approx -150^\circ; \psi \approx 155^\circ$; $\varphi \approx -90^\circ; \psi \approx 155^\circ$
Val3	2	$\varphi \approx 110^\circ; \psi \approx -30^\circ$; $\varphi \approx 50^\circ; \psi \approx -30^\circ$	Dpg3	1	$\varphi \approx -55^\circ; \psi \approx 180^\circ$	Deg3	1	$\varphi \approx -60^\circ; \psi \approx 180^\circ$
Tyr4	1	$\varphi \approx 100^\circ; \psi \approx -55^\circ$	Tyr4	2	$\varphi \approx -75^\circ; \psi \approx 165^\circ$; $\varphi \approx -75^\circ; \psi \approx 130^\circ$	Tyr4	2	$\varphi \approx -85^\circ; \psi \approx -50^\circ$; $\varphi \approx -125^\circ; \psi \approx -50^\circ$
Ile5	1	$\varphi \approx 98^\circ; \psi \approx -60^\circ$	Aib5	1	$\varphi \approx 60^\circ; \psi \approx -170^\circ$	Aib5	1	$\varphi \approx -50^\circ; \psi \approx 140^\circ$
His6	2	$\varphi \approx 30^\circ; \psi \approx -28^\circ$; $\varphi \approx 100^\circ; \psi \approx -28^\circ$	His6	1	$\varphi \approx -145^\circ; \psi \approx 150^\circ$	His6	1	$\varphi \approx -150^\circ; \psi \approx 150^\circ$
Pro7	1	$\varphi \approx 105^\circ; \psi \approx 145^\circ$	Pro7	1	$\varphi \approx -75^\circ; \psi \approx -25^\circ$	Pro7	1	$\varphi \approx -150^\circ; \psi \approx 155^\circ$
Phe8	1	$\varphi \approx 30^\circ; \psi \approx -35^\circ$	Dpg8	1	$\varphi \approx 180^\circ; \psi \approx -25^\circ$	Dpg8	1	$\varphi \approx -75^\circ; \psi \approx -20^\circ$

* The conformers of AngII were identified in a previous work.³⁶

sequences can decrease the standard entropy of association with the At1 receptor, by decreasing the number of backbone conformers, without significant changes in the average structure.

The synthesis of some of the designed analogs is currently under development in the Chemistry Department of the University of Minho.

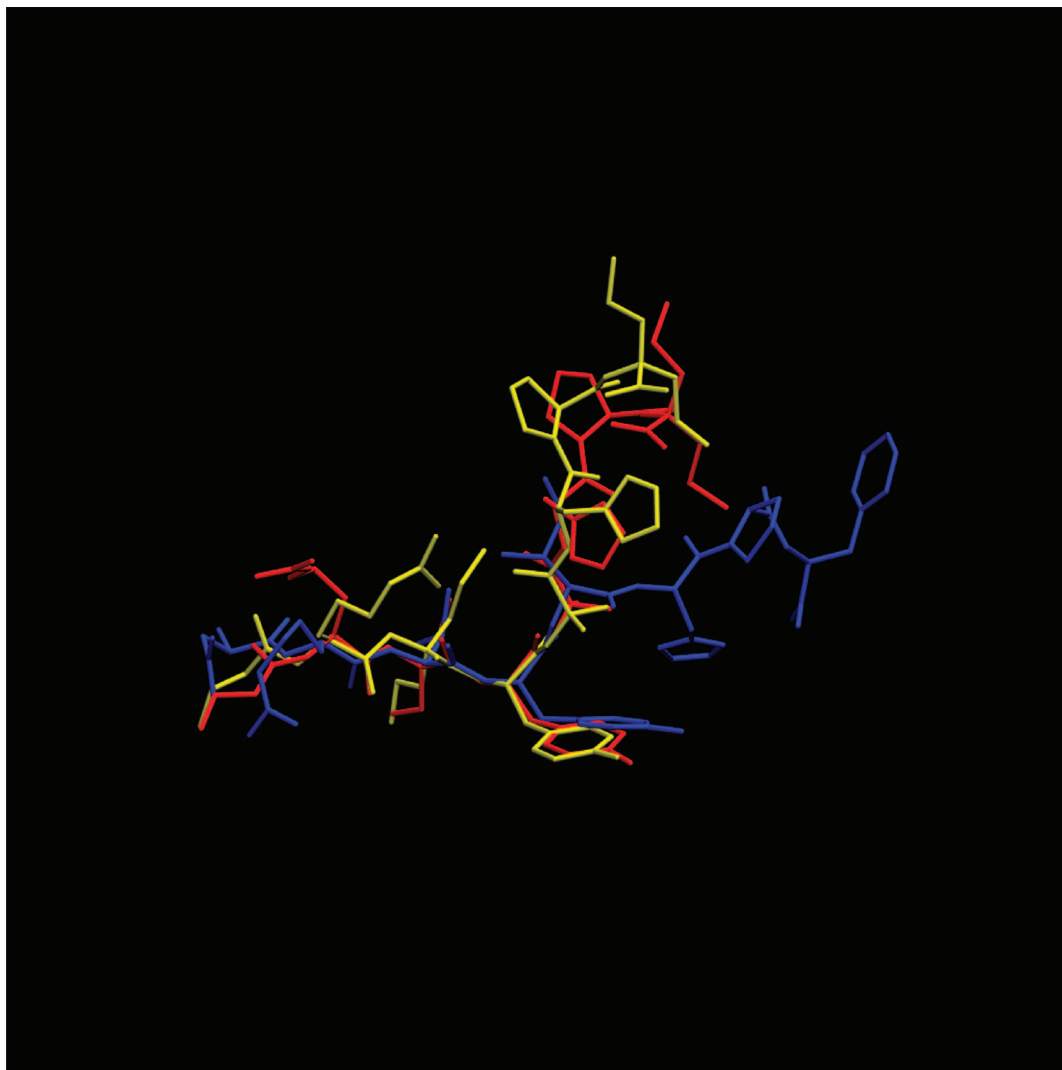


Figure 5. Superimposition of the N-terminal portions of minimal energy found structures of AngII (blue), Comp11 (yellow) and Comp13 (red). Only the N-terminal backbone atoms were used as reference for the superimposition. Hydrogens were omitted for simplicity of representation.

Acknowledgment. This work was supported by Fundação para a Ciência e Tecnologia (FCT) project POCI/QUI/55673/2004. The collaboration of Prof. Mavramoustakos is greatly appreciated for supplying us with their AngII structure in DMSO, obtained through NMR spectroscopy data.

Supporting Information Available: A set of tables that was too extensive to be included in the article: Table S1 has a list of the simulated species and their initial setup conditions for the performed simulations. Tables S2 and S3 contain data regarding the distances $C\alpha_i-C\alpha_{i+2}$ and $C\alpha_i-C\alpha_{i+3}$, respectively, including maximum, minimum and average values for every possibility. Some relevant data collected from each performed simulation. These data are presented in the following order: substance name; backbone dihedral charts with the representation of (one for each residue) angle vs simulation time, ϕ vs ψ ; population chart (population distribution of each backbone dihedral during the complete simulation); distances between $C\alpha$ of residue i and Ca of residue $i + 2$; distances between $C\alpha$ of residue i and Ca of residue $i + 3$; distance between $H(\text{residue } 4)-N(\text{residue } 6)$, $H(\text{residue } 6)-O1(\text{residue } 8)$ and $H(\text{residue } 6)-O2(\text{residue } 8)$ vs simulation time; angle $O(\text{residue } 4)-H(\text{residue } 4)-H(\text{residue } 6)$ vs simulation time; angle $N(\text{residue } 6)-H(\text{residue } 6)-O1(\text{residue } 8)$ vs simulation time; angle $N(\text{residue } 6)-H(\text{residue } 6)-O2(\text{residue } 8)$ vs simulation time; figures showing backbone structure superimposed from residue 4 to residue 6, where side chains and hydrogen atoms are not shown (upper left position), conformer with the minimal found energy, where hydrogen atoms are not shown (upper right position), superimposition of residue 2 side chain, showing the relative disposition of the side chains of residue 1 and residue 4, where hydrogen atoms are omitted (lower left position), superimposition of residue 6 side chain, showing the relative disposition of residue 4's side chain and residue 8, where hydrogen atoms are omitted (lower right position). This material is available free of charge via the Internet at <http://pubs.acs.org>.

8) vs simulation time; figures showing backbone structure superimposed from residue 4 to residue 6, where side chains and hydrogen atoms are not shown (upper left position), conformer with the minimal found energy, where hydrogen atoms are not shown (upper right position), superimposition of residue 2 side chain, showing the relative disposition of the side chains of residue 1 and residue 4, where hydrogen atoms are omitted (lower left position), superimposition of residue 6 side chain, showing the relative disposition of residue 4's side chain and residue 8, where hydrogen atoms are omitted (lower right position). This material is available free of charge via the Internet at <http://pubs.acs.org>.

References and Notes

- (1) Hruby, V. J. *Nat. Rev. Drug Disc.* **2002**, *1*, 847–858.
- (2) Mavromoustakos, T.; Kolocouris, A.; Zervou, M.; Roumelioti, P.; Matsoukas, J.; Weisemann, R. *J. Med. Chem.* **1999**, *42*, 1714–1722.
- (3) Spyroulias, G. A.; Nikolakopoulou, P.; Tzakos, A.; Gerothanassis, I. P.; Magafa, V.; Manessi-Zoupa, E.; Cordopatis, P. *Eur. J. Biochem.* **2003**, *270*, 2163–2173.
- (4) Müller-Nordhorn, J.; Willich, S. *Herz* **2003**, *28*, 733.
- (5) Kaschina, E.; Unger, T. *Blood Pressure* **2003**, *12*, 70–88.
- (6) Zorba Paster, R.; Snively, D. B.; Sweet, A. R.; Draper, R. A.; Goldberg, A. I.; Soffer, B. A.; Sweet, C. S. *Clin. Ther.* **1998**, *20*, 978.
- (7) Berl, T. *J. Am. Soc. Nephrol.* **2004**, *15*, S71–76.
- (8) Gurrath, M. *Curr. Med. Chem.* **2001**, *8*, 1605–1648.

- (9) Moutevelis-Minakakis, P.; Gianni, M.; Stougiannou, H.; Zoumpoulakis, P.; Zoga, A.; Vlahakos, A. D.; Iliodromitis, E.; Mavromoustakos, T. *Bioorg. Med. Chem. Lett.* **2003**, *13*, 1737.
- (10) Duncia, J. V.; Carini, D. J.; Chiu, A. T.; Johnson, A. L.; Price, W. A.; Wong, P. C.; Wexler, R. R.; Timmermans, P. B. M. W. *Med. Res. Rev.* **1992**, *12*, 149–191.
- (11) Tzakos, A. G.; Gerothanassis, I. P.; Troganis, A. N. *Curr. Topics Med. Chem.* **2004**, *4*, 431.
- (12) Costa, S. P. G.; Maia, H. L. S.; Pereira-Lima, S. M. M. A. *Org. Biomol. Chem.* **2003**, *1*, 1474–1479.
- (13) Jiang, W.-Q.; Costa, S. P. G.; Maia, H. L. S. *Org. Biomol. Chem.* **2003**, *1*, 3804–3810.
- (14) Preto, M. A. C.; Melo, A.; Costa, S. P. G.; Maia, H. L. S.; Ramos, M. J. *J. Phys. Chem. B* **2003**, *107*, 14556–14562.
- (15) Preto, M. A. C.; Melo, A.; Costa, S. P. G.; Maia, H. L. S.; Ramos, M. J. *Modelling of bioactive peptides with inclusion of synthetic amino acids*; 27th European Peptide Symposium, Sorrento, Italy, 2002.
- (16) Hsieh, K.-H.; Kiraly-Olah, I. C.; Jorgensen, E. C.; Lee, T. C. *J. Med. Chem.* **1979**, *22*, 1044–1047.
- (17) Bovy, P. R.; O'Neal, J. M.; Olins, G. M.; Patton, D. R.; McMahon, E. G.; Palomo, M.; Koepke, J. P.; Salles, K. S.; Trapani, A. J.; et al. *J. Med. Chem.* **1990**, *33*, 1477–1482.
- (18) Wilkes, B. C.; Masaro, L.; Schiller, P. W.; Carpenter, K. A. *J. Med. Chem.* **2002**, *45*, 4410–4418.
- (19) Roumelioti, P.; Tselios, T.; Alexopoulos, K.; Mavromoustakos, T.; Kolocouris, A.; Moore, G. J.; Matsoukas, J. M. *Bioorg. Med. Chem. Lett.* **2000**, *10*, 755.
- (20) Matsoukas, J.; Cordopatis, P.; Belte, U.; Goghari, M. H.; Ganter, R. C.; Franklin, K. J.; Moore, G. J. *J. Med. Chem.* **1988**, *31*, 1418–1421.
- (21) Samanen, J.; Cash, T.; Narindray, D.; Brandeis, E.; Adams, W.; Weideman, H.; Yellin, T.; Regoli, D. *J. Med. Chem.* **1991**, *34*, 3036–3043.
- (22) Turk, J.; Needleman, P.; Marshall, G. R. *Mol. Pharmacol.* **1976**, *12*, 217–224.
- (23) Matsoukas, J. M.; Goghari, M. H.; Scanlon, M. N.; Franklin, K. J.; Moore, G. J. *J. Med. Chem.* **1985**, *28*, 780–783.
- (24) Case, D. A.; Pearlman, D. A.; Caldwell, J. W.; Cheatham, T. E. I.; Ross, W. S.; Simmerling, C. L.; Darden, T. A.; Merz, K. M.; Stanton, R. V.; Cheng, A. L.; Vicent, J. J.; Crowley, M.; Tsui, V.; Radmer, R. J.; Duan, Y.; Pitera, J.; Massova, I.; Seibel, G. L.; Singh, U. C.; Weiner, P. K.; Kollman, P. A. *Amber 6*; University of California: San Francisco, CA, 1999.
- (25) Cornell, W. D.; Cieplak, P.; Bayly, C. I.; Gould, I. R.; Merz, K. M.; Ferguson, D. M.; Spellmeyer, D. C.; Fox, T.; Caldwell, J. W.; Kollman, P. A. *J. Am. Chem. Soc.* **1995**, *117*, 5179–5197.
- (26) Gould, I. R.; Cornell, W. D.; Hillier, I. H. *J. Am. Chem. Soc.* **1994**, *116*, 9250–9256.
- (27) Skaf, M. S. *J. Chem. Phys.* **1997**, *107*, 7996–8003.
- (28) Matsoukas, J. M.; Hondrelis, J.; Keramida, M.; Mavromoustakos, T.; Makriyannis, A.; Yamdagni, R.; Wu, Q.; Moore, G. J. *J. Biol. Chem.* **1994**, *269*, 5303–5312.
- (29) JoslAae Mario Martínez, L. M. *J. Comput. Chem.* **2003**, *24*, 819–825.
- (30) Berendsen, H. J. C.; Postma, J. P. M.; Gunsteren, W. F. v.; DiNola, A.; Haak, J. R. *J. Chem. Phys.* **1984**, *81*, 3684–3690.
- (31) Wilfred, F.; van.Gunsteren, H. J. C. B. *Angew. Chem., Int. Ed. Engl.* **1990**, *29*, 992–1023.
- (32) Ryckaert, J.-P.; Ciccotti, G.; Berendsen, H. J. C. *J. Comput. Phys.* **1977**, *23*, 327.
- (33) Ulrich, E.; Lalith, P.; Max, L. B.; Tom, D.; Hsing, L.; Lee, G. P. *J. Chem. Phys.* **1995**, *103*, 8577–8593.
- (34) Darrin, M. Y.; Tom, A. D.; Lee, G. P. *J. Chem. Phys.* **1993**, *99*, 8345–8348.
- (35) Humphrey, W.; Dalke, A.; Schulten, K. *J. Mol. Graph.* **1996**, *14*, 33.
- (36) Preto, M. A. C.; Melo, A.; Maia, H. L. S.; Mavromoustakos, T.; Ramos, M. J. *J. Phys. Chem. B* **2005**, *109*, 17743–17751.
- (37) Mohan, R.; Chou, Y. L.; Bihovsky, R.; Lumma, W. C.; Erhardt, P. W.; Shaw, K. J. *J. Med. Chem.* **1991**, *34*, 2402–2410.